Int J Cardiovasc Imaging (2016) 32:1595–1604
DOI 10.1007/s10554-016-0936-7

ORIGINAL PAPER

Fluorescent lifetime imaging microscopy using Europium complexes improves atherosclerotic plaques discrimination

Letícia Bonfante Sicchieri[1] · Rodrigo de Andrade Natal[2] · Lilia Coronato Courrol[1,3]

Received: 27 April 2016 / Accepted: 5 July 2016 / Published online: 13 July 2016

Abstract The objective of this study is to characterize arterial tissue with and without atherosclerosis by fluorescence lifetime imaging microscopy (FLIM) using Europium Chlortetracycline complex (EuCTc) as fluorescent marker. For this study, twelve rabbits were randomly divided into a control group (CG) and an experimental group (EG), where they were fed a normal and hypercholesterolemic diet, respectively, and were treated for 60 days. Cryosections of the aortic arch specimens were cut in a vertical plane, mounted on glass slides, and stained with Europium (Eu), Chlortetracycline (CTc), Europium Chlortetracycline (EuCTc), and Europium Chlortetracycline Magnesium (EuCTcMg) solutions. FLIM images were obtained with excitation at 405 nm. The average autofluorescence lifetime within plaque depositions was ~1.36 ns. Reduced plaque autofluorescence lifetimes of 0.23 and 0.31 ns were observed on incubation with EuCTc and EuCTcMg respectively. It was observed a quenching of collagen, cholesterol and TG emission spectra increasing EuCTc concentration. The drastic reduction in fluorescence lifetimes is due to a resonant energy transfer between collagen, triglycerides, cholesterol and europium complexes, quenching fluorescence.

✉ Lilia Coronato Courrol
lccourrol@gmail.com

[1] Center of Lasers and Applications, Institute of Energy and Nuclear Research, São Paulo University, São Paulo, Brazil

[2] Departments of Pathology, Faculty of Medical Sciences, State University of Campinas, Campinas, São Paulo, Brazil

[3] Department of Exact and Earth Sciences, Federal University of São Paulo, Diadema, São Paulo, Brazil

Keywords Atherosclerosis · FLIM · Europium Chlortetracycline · FRET · Collagen · Cholesterol · Triglycerides

Introduction

Atherosclerosis is a form of arteriosclerosis characterized by the presence of the atheroma plaque, an accumulation of degenerative material in the intima layer of artery walls [1]. The plaque contains macrophage cells, lipids, calcium, and a variable amount of fibrous connective tissue [2]. The accumulated material narrows the artery walls and restricts blood flow [3]. Despite medical advances, atheroma rupture events continue to be major contributors to the cardiovascular death toll every year.

As a result of technological advances, the number of available non-invasive cardiovascular imaging techniques have increased substantially over the last decade [4]. Various non-invasive imaging cardiac tests can be listed including computer tomography (CT) [5], magnetic resonance imaging (MRI) [6], positron emission tomography (PET) [7], nuclear single-photon emission computed tomography (SPECT), echocardiography and intravascular ultrasound (IVUS) [8], among others. Some of these imaging examinations require the use of intravenous contrast administration, that should be avoided in patients with abnormal kidney function [9]. Besides, overweight patients may present lower image quality for tests as stress echocardiogram, SPECT and PET [10].

Several new optical imaging techniques do not require any kind of contrast and are being developed for the identification of plaques that have a high-risk of rupture [11–15]. Fluorescence lifetime imaging microscopy (FLIM) has been developed as an extension of the time-resolved fluorescence

spectroscopy (TRFS) technique to provide images of time-resolved properties that map the biochemical composition of regions of arteries with high spatial resolution. Fluorescence has been used to study the biochemical composition of arteries since the 1960s. TRFS techniques are sensitive in detecting collagen cross-links, as well as identifying macrophages and lipid-rich content [16–19]. A few studies have successfully demonstrated a plaque characterization technique with FLIM images of the human aorta (collagen, lipid, and elastin content) [11, 16, 20, 21].

There are several types of autofluorescent lipids, lipoproteins, and lipopigments present in plaque. Elastin has an average fluorescence lifetime of 1.9 ns at 380 nm [22]. Collagen I has longer lifetimes of 5.2 ns at its emission peak of 390 nm, and 4.5 ns at 460 nm [23]. Lipids have short lifetimes (<1.8 ns) across the emission spectrum [24]. Lipid-laden macrophages (foam cells) exhibit short average fluorescence lifetimes based on lipid content [24]. Some plaque fluorophores fluoresce at emission wavelengths similar to collagen and elastin, such as low-density lipoproteins (LDL) and very low-density lipoproteins (VLDL), shortening the average fluorescence lifetimes at these wavelength bands, but others, such as ceroid, have a fluorescence emission peak at longer wavelengths [25, 26].

Lindgren and Raekallioll [27] observed that tetracycline binds selectively to atheroma when administered orally in therapeutic concentrations. Moreover, tetracycline was located in the same area of the atheroma as the phospholipid stains, suggesting that it is lipophilic. Golub et al. [28] observed that the non-antibacterial properties of Tetracyclines (TCs), could have therapeutic potential in cardiovascular diseases.

Chlortetracycline is a member of the tetracycline group of broad-spectrum antimicrobial drugs used to treat bacterial infections in animals [29–31]. The tetracyclines are strong chelating agents. Europium trivalent ions can form complexes with tetracyclines [32–38]. When Europium tetracycline is excited in a wavelength resonant with the tetracyclines absorption band, europium ion luminescence can be observed due to the ligand large absorption and an antenna-effect [35] that transfers the absorbed energy to the europium through an intramolecular process. The ion luminescence is also enhanced by the isolation that the ligand provides from the water molecules, preventing energy transfer to them. The Europium-Chlortetracycline complex (EuCTc) has an absorption band centered at 400 nm, emission at ~617 nm and a large Stokes-shift (approximately 210 nm). Europium-Chlortetracycline complex was used to mark the formation of atherosclerotic plaque induced on rabbits fed with 1 % cholesterol [39, 40]. In this study, aortas stained with Europium (Eu), Chlortetracycline (CTc), the EuCTc complex and EuCTc in the presence of Magnesium (EuCTcMg) were studied by FLIM in an attempt to characterize a new marker for atherosclerosis.

Materials and methods

Animal experimentation

Twelve New Zealand rabbits were divided in two groups: (a) experimental group (EG) with nine animals and (b) a control group (CG) with three animals.

The animals in the EG received a diet with 1 % of cholesterol (Sigma) and the animals of the CG received a normal diet. The growth of atherosclerotic plaque was accompanied during 60 days [41]. The protocol was approved by the Ethics Committee of UNIFESP (Protocol nº 0327/12).

After 60 days, the aortic arch of the animals from both CG and EG groups was cut in the vertical plane at 6 μm thickness on a cryostat, then mounted on glass slides and stained with Oil Red, Europium (Eu), Chlortetracycline (CTc), Europium-Chlortetracycline (EuCTc) and EuCTcMg.

Solutions

The CTc solution was prepared in milliQ water with 21 μM, and the Europium solution with 31.5 μM.

The EuCTc complex was prepared in 10 mmol/L 3-(N-Morpholino) propanesulfonic acid (Mops, from Carl Roth) of pH 6.9, with the molar ratio 1.5 Eu:1.0 CTc, and the EuCTcMg was prepared with the molar ratio 1.5 Eu:1.0 CTc and Magnesium with 0.75 mM. The ratio of EuCTc:Mg was 1:1. It was observed that EuCTcMg present higher emission intensity in the presence of oxidized low density lipoprotein (LDL) as compared to the emission of EuCTc (data not published).

Collagen solution was prepared with hydrolyzed collagen (Stem Pharmaceuticals) dissolved in milliQ water in a concentration of 1 g/L. Triglycerides (TG) solution (TGML-5515) and Cholesterol solution (CHSL-5710) were obtained from Elitech Clinical Systems.

Instrumentation

The absorption spectra were obtained using a Shimadzu MultiSpec-1500 spectrophotometer. The emission spectra were obtained by exciting the samples at 400 nm using a 1 mm optical path cuvette (Hellma). The sample fluorescence was measured in the range 415–780 nm using a RF-5301 (Shimadzu Scientific Instruments).

The fluorescence lifetimes were obtained with a pulsed diode laser ($\lambda = 403$ nm) and driver (PDL 800-B) from Picoquant, with a repetition rate of 8 MHz. Detection was performed by a photomultiplier (Hamamatsu PMA 182-PM)

and a long-pass colored glass filter RG495 and a reflective ND filter ND30A. Data were processed by PicoQuant PicoHarp 300 and then analyzed using OriginLab Software. For the FLIM images the samples were investigated in the National Institute of Science and Technology on Photonics Applied to Cell Biology (INFABIC), at the State University of Campinas. It was used a 40×/1.3 NA oil immersion EC Plan-Neofluar objective on a Confocal Upright LSM780 NLO device (Carl Zeiss AG, Germany) equipped with a Becker–Hickl TCSPC FLIM system. FLIM was excited with a 405 nm diode laser (BDL-405-SMC, Becker & Hickl) with 65 ps pulses and 80 MHz repetition rate, the emission was collected above 415 nm using a filter FF02-409/LP-25. Each region with 177×177 µm (256×256 pixels) was excited for 120 s at a rate of $\approx 1 \times 10^5$ ph/s and detected with the Becker & Hickl, PMH-100 detector. The images were analyzed with the software SPCImage5.0 and the quality fits were chosen based on the reduced Chi square statistic. The distributions of lifetimes were analyzed from the images and the best fit was obtained with two-exponentials, and the average lifetime was obtained with the following formula:

$$\tau = \frac{\sum_i A_i t_i}{\sum_i A_i}$$

where t_i and A_i are lifetime and pre-exponential factor of the i-esime decay component.

Results

FLIM images for aorta stained with Eu, CTc, EuCTc and EuCTcMg

The aorta slices obtained for the animals from the control and experimental groups were stained with Oil red, Eu, CTc, EuCTc and EuCTcMg, and both media and intima layers images were obtained by the FLIM technique and compared with the aortas that were not stained. The images are shown in Fig. 1.

Figure 2a, shows the lifetime histograms correspondent to each image shown in Fig. 1b, for media and intima layers autofluorescence lifetimes and fluorescence lifetimes obtained in slices of media and intima layers stained with Eu, CTc, EuCTc and EuCTcMg. The normalized FLIM-derived fits are shown in the Fig. 2b.

Average FLIM-derived parameters are provided in Table 1. For control group aortas, media layer autofluorescences were identified by longer lifetimes compared to intima layer regions 1.52 ns versus 1.31 ns, respectively. The lifetime reduces from 1.46 to 1.25 by staining the media layer with Eu. For experimental group aortas as well, the media layer autofluorescences were identified by longer lifetimes compared to intima layer regions 1.62 and 1.36 ns, respectively. The lifetimes are similar in media layer stained with Eu or CTc. The lifetimes are shorter in the case of intima layers stained with Eu (1.08 ns) and CTc (1.13 ns).

The incubation with EuCTc and EuCTcMg promotes a decrease in the lifetimes in both media and intima layer for control groups 1.24 ns media and 1.02 ns intima (EuCTc) and 1.47 ns media and 1.20 ns intima (EuCTcMg), respectively. A drastic decrease in fluorescence lifetimes for experimental groups media and intima layers was observed 0.86 ns media and 0.23 ns intima (EuCTc) and 0.71 ns media and 0.31 ns intima (EuCTcMg) respectively. Table 2 enlists the fit parameters obtained for aleatory points taken in each image shown in Fig. 1.

Spectral and temporal profile of tissue fluorophores in the presence of EuCTc

To understand the differences in FLIM parameter obtained in slices of media and intima layers stained with EuCTc, shown in "FLIM images for aorta stained with Eu, CTc, EuCTc and EuCTcMg", some aorta fluorophores spectroscopic properties were studied in the presence of EuCTc.

Figure 3a shows absorption spectra of CTc, EuCTc and the media and intima layers of the atherosclerotic aorta [42]. It is observed that EuCTc has a large absorption band centered at 400 nm, resonant with the main aorta absorption peak. This absorption band is due to the presence of the chlortetracycline ligand, which in its uncomplexed form has a slightly blue shifted absorption spectrum.

Figure 3b shows the emission of CTc, EuCTc, collagen, cholesterol and triglycerides (TG), obtained with excitation at 400 nm. The emission spectrum of EuCTc shows evident Eu(III) characteristic peaks at 580, 591, 617 and assignable to $^5D_0 \rightarrow {}^7F_j$ (j = 0–2), respectively. Collagen and cholesterol present large emission bands around 460 nm and TG presents emission band at 530 nm coincident with CTc emission.

The changes in the spectral and temporal evolutions of collagen, cholesterol and TG solutions emission bands, excited at 400 nm, in the presence of variable amounts of EuCTc (added from 100 to 900 µL in 1 mL of each solution), were measured and results are shown in Fig. 4.

In Fig. 4a it is possible to see a decrease in the collagen emission band around 462 nm with a raise in the EuCTc concentration and simultaneously an enhancement in the Eu emission band around 617 nm, indicating an energy transfer process between collagen and EuCTc. Blue emission of collagen was attributed to tyrosine and dityrosine while the yellow-green fluorescence was assigned to pentosidine, formed in vivo via a Maillard reaction involving pentose lysine and arginine [43]. In Fig. 4b it is observed a decrease in the collagen emission lifetime in the presence of EuCTc.

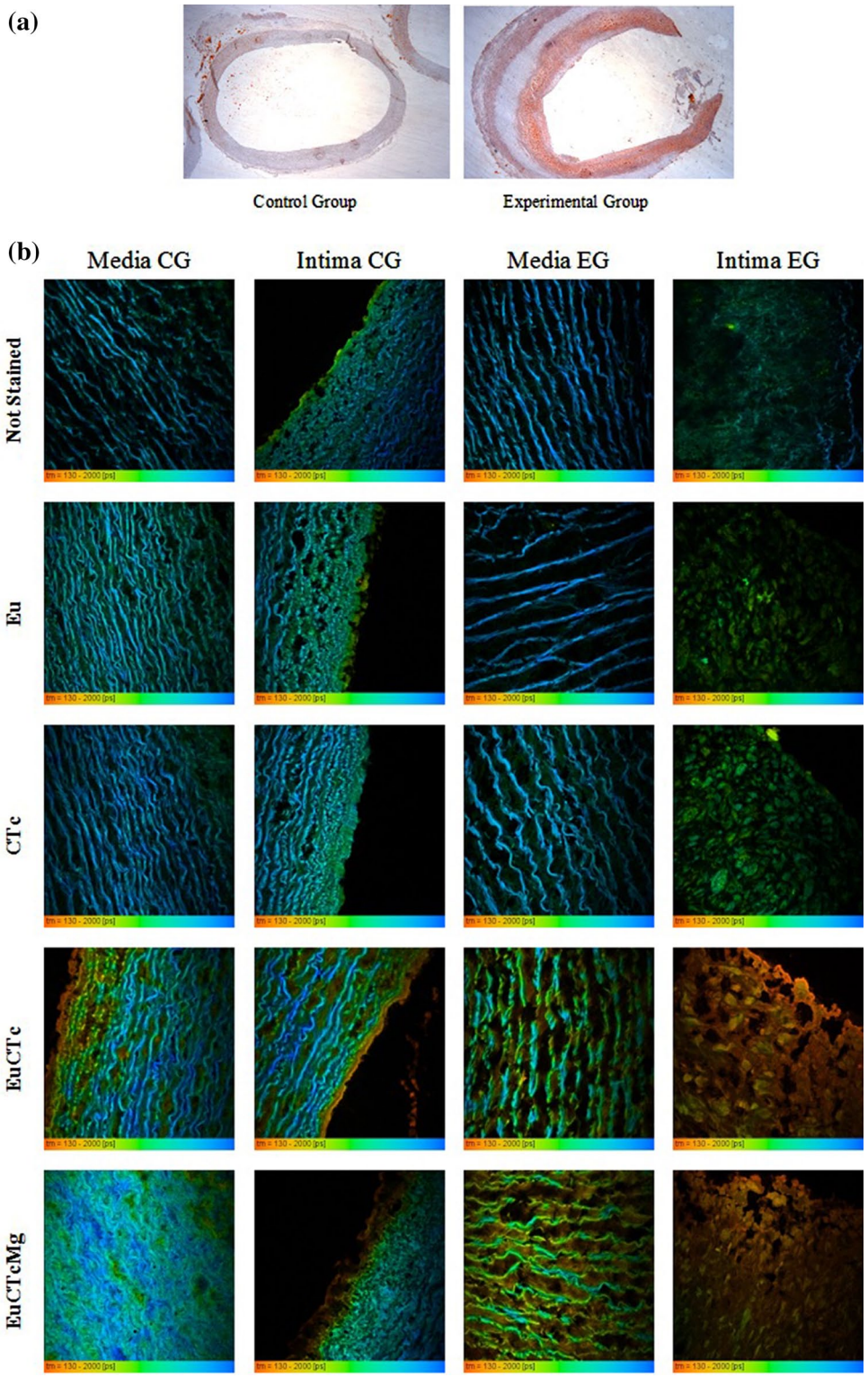

Fig. 1 **a** Cross section of artery of animal of 60 days diet stained with Oil red: Control Group and Experimental Group. **b** Images of media and intima layers autofluorescence not stained and stained with Eu, CTc, EuCTc and EuCTcMg, and both media and intima layers

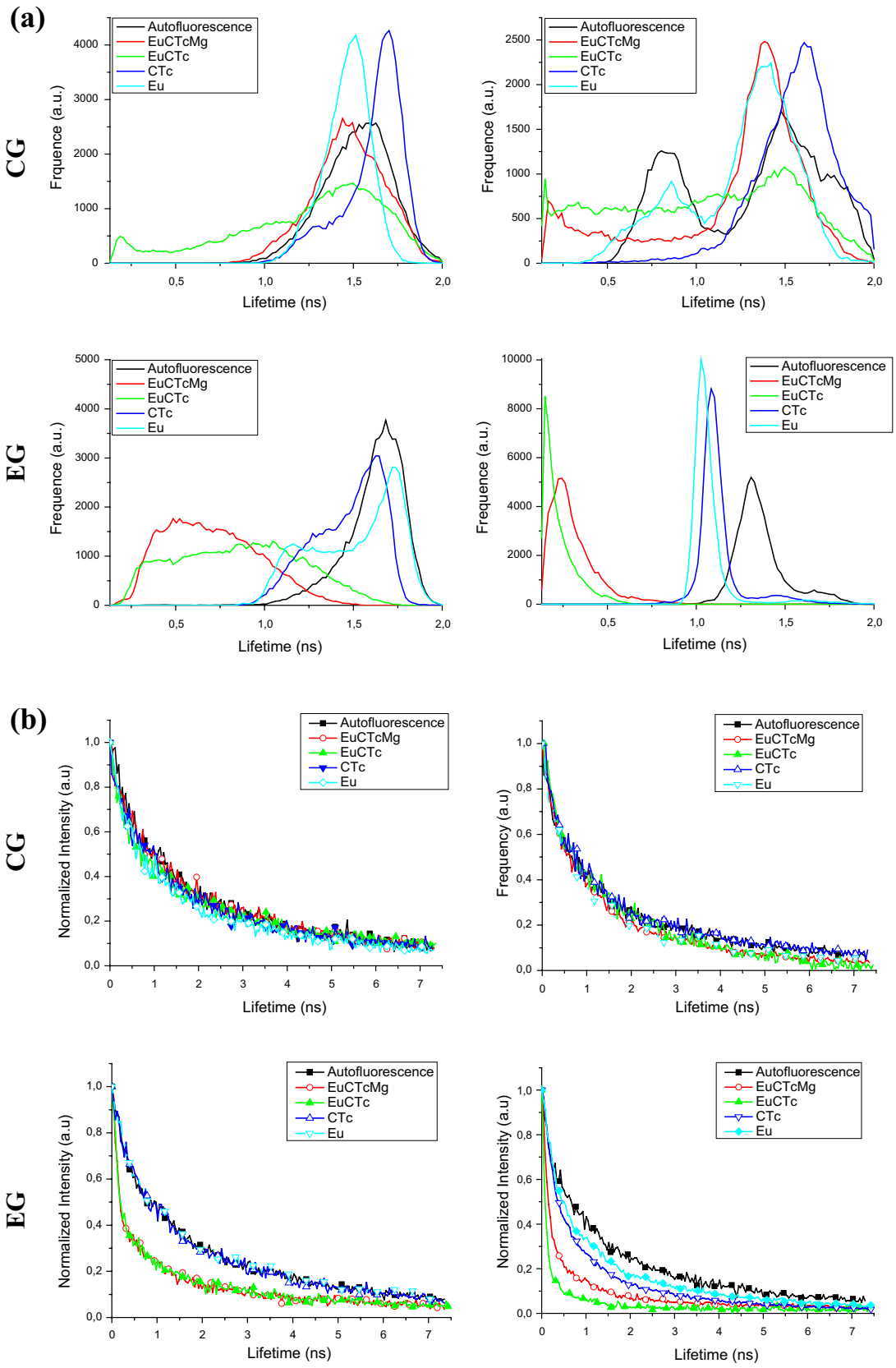

Fig. 2 **a** Lifetime histograms correspondent to each image shown in Fig. 1, the y axis represents the frequency. **b** Normalized FLIM-derived fits

Table 1 Fitting parameters for the media and intima fluorescence lifetime decays obtained with a two-exponential function: average lifetimes (ps) and reliability range (a) given by the program ranging over all the image

	Media	Intima
CG	Not stained: 1.52 (1.32–1.70)	Not stained: 1.31 (0.80–1.68)
	EuCTcMg: 1.47 (1.27–1.67)	EuCTcMg: 1.20 (0.41–1.50)
	EuCTc: 1.24 (0.70–1.62)	EuCTc: 1.02 (0.37–1.55)
	CTc: 1.61 (1.37–1.74)	CTc: 1.60 (1.37–1.84)
	Eu: 1.46 (1.32–1.58)	Eu: 1.25 (0.81–1.51)
EG	Not stained: 1.62 (1.44–1.76)	Not stained: 1.36 (1.25–1.52)
	EuCTcMg: 0.71 (0.44–1.00)	EuCTcMg: 0.31 (0.20–0.45)
	EuCTc: 0.86 (0.46–1.23)	EuCTc: 0.23 (0.15–0.35)
	CTc: 1.47 (1.23–1.65)	CTc: 1.13 (1.05–1.23)
	Eu: 1.51 (1.18–1.75)	Eu: 1.08 (1.01–1.15)

The cholesterol emission band at 470 nm was obtained upon excitation at 400 nm as seen in Fig. 4c. With increase in concentrations of EuCTc, a large band around 524 nm, corresponding to CTc emission, is observed concomitantly with an increase in the Europium emission band. This fact indicates a strong energy transfer between cholesterol and CTc. In the Fig. 4d it is observed a decrease in cholesterol emission lifetime with increase of EuCTc concentration in the solution.

Apparently TG emission bands show less changes in the presence of EuCTc as shown in Fig. 4e. But important changes in TG decay kinetics in the presence of EuCTc are observed in Fig. 4f.

Figure 4g shows the evolution of the averaged lifetimes (the best fits were obtained by two-exponential functions) of collagen, cholesterol and TG in function of the presence of variable amounts of EuCTc. Comparing collagen, cholesterol ant TG lifetimes without EuCTc and with the addition of 900 µl of EuCTc, collagen lifetime decreases 42 %, cholesterol 39 % and TG 60 %.

Discussion

Here we studied the FLIM images obtained with excitation at 405 nm of aortas stained with Eu, CTc, EuCTc and EuCTcMg. An important difference between the intima fluorescence lifetime of normal aorta (1.02 ns) and atherosclerotic aorta (0.23 ns) can be noted in aortas stained with EuCTc.

The influence of the presence of EuCTc in the aorta fluorophores collagen, cholesterol and TG solutions was examined. It was observed a quenching of collagen, cholesterol and TG emission spectra increasing EuCTc concentration.

It was identified a Förster resonance energy transfer (FRET) between collagen, and Europium complexes, quenching residual collagen fluorescence. In addition, cholesterol and TG emissions are transferred to the EuCTc complex. Other fluorophores not identified in this paper, as vitamins, beta-carotene, lipoproteins, etc, can also transfer energy to EuCTc. These fluorophores (donors) must exhibit a significant emission spectrum overlap with the acceptor's excitation spectrum (EuCTc or EuCTcMg).

FRET is a process by which a fluorophore (the donor, here collagen, cholesterol or TG) in an excited state transfers its energy to a neighboring molecule (the acceptor, here EuCTc) by nonradiative dipole–dipole interaction. When FRET occurs, the donor emission is decreased and the acceptor emission is increased [44]. In the presence of FRET, the donor average lifetime decreases as the fast-acting energy transfer siphons off photonic energy [45].

Since several fluorophores, such as cholesterol and TG, are present in higher concentrations in the intima layer, the energy transfer effect to EuCTc in this layer is more important than in the media layer.

With the addition of EuCTc to TG, collagen and cholesterol solutions it is observed a decrease of these molecules emission lifetimes, and this effect is more pronounced in TG. This can be seen in Fig. 4g. This result shows that the greatest energy transfer occurs from TG to the EuCTc complex.

It is known that in rabbits very low density lipoproteins (VLDL) present an important role in the formation of the plaque [46]. Triglyceride is transported by the plasma in (VLDL) and secreted from the liver and intestine. Most of these triglycerides is rapidly and irreversibly removed from the VLDL, but a small amount also appears in the plasma low density lipoproteins (LDL) as a consequence of the catabolic conversion of VLDL to LDL. The VLDL is the lipoprotein with the highest TG concentration. Therefore, the detection of TG in atherosclerotic lesions is important for understanding the mechanisms of atherogenesis and growth of atherosclerotic lesions [47].

We observed also a strong energy transfer mechanism between cholesterol and EuCTc, the main constituent of low density lipoprotein (LDL), that can result in the reduction of emission lifetime in the intima layer compared with the media layer.

In the human aorta, interstitial collagen type I is abundant in the intima and the proportion of type I to type III tends to increase with atheromatous changes [43]. Collagen is the most abundant protein in animals and its function is to hold different organs in place and together [48]. Our results shows that the Europium Chlortetracycline complex has a

Table 2 Fitting parameters for the media and intima fluorescence lifetime decays obtained taking a specified point in the image: lifetimes (τ_i in ns), normalized pre-exponential factors (A_i) and average lifetimes (τ in ns) for autofluorescence, Eu, CTc, EuCTc and EuCTcMg

Not stained	CG media	EG media	CG INTIMA	EG INTIMA					
A1	0.33±0.04	0.33±0.02	0.36±0.02	0.61±0.01					
t1 [ns]	0.38±0.06	0.29±0.02	0.32±0.03	1.76±0.05					
A2	0.63±0.03	0.61±0.01	0.54±0.02	0.31±0.02					
t2 [ns]	2.32±0.20	2.19	2.10±0.12	0.22±0.02					
τ [ns]	**1.64**	**1.52**	**1.39**	**1.24**					
R2	0.98	0.99	0.99	0.99					
Eu	CG MEDIA	EG MEDIA	CG INTIMA	EG INTIMA	CTc	CG MEDIA	EG MEDIA	CG INTIMA	EG INTIMA
A1	0.51±0.03	0.37±0.03	0.40±0.03	0.52±0.01	A_1	0.23±0.03	0.51±0.03	0.55±0.03	0.60±0.01
t1 [ns]	2.21±0.20	0.44±0.05	2.33±0.23	0.31±0.01	t_1 [ns]	0.32±0.07	2.67±0.27	1.99±0.14	0.28±0.01
A2	0.43±0.03	0.55±0.03	0.53±0.03	0.47±0.01	A_2	0.63±0.03	0.41±0.04	0.41±0.03	0.42+0.01
t2 [ns]	0.39±0.04	2.46±0.20	0.44±0.03	1.75±0.06	t_2 [ns]	1.92±0.13	0.49±0.05	0.31±0.04	1.55±0.04
τ [ns]	**1.38**	**1.65**	**1.24**	**1.00**	τ [ns]	**1.48**	**1.71**	**1.27**	**0.81**
R2	0.99	0.99	0.99	0.99	R^2	0.98	0.99	0.99	0.99
EuCTc	CG MEDIA	EG MEDIA	CG INTIMA	EG INTIMA	EuCTcMg	CG MEDIA	EG MEDIA	CG INTIMA	EG INTIMA
A1	0.57±0.02	0.67±0.01	0.42±0.02	0.87±0.01	A_1	0.61±0.02	0.34±0.01	0.35±0.02	0.764±0.009
t1 [ns]	1.98±0.10	0.143±0.006	0.28±0.03	0.087±0.001	t_1 [ns]	2.49±0.19	1.53±0.07	0.28±0.02	0.141±0.009
A2	0.34±0.02	0.325±0.009	0.64±0.02	0.135±0.001	A_2	0.32±0.03	0.66±0.01	0.61±0.02	0.245±0.009
t2 [ns]	0.22±0.03	1.70±0.08	2.17±0.11	0.87±0.05	t_2 [ns]	0.38±0.05	0.134±0.006	1.65±0.05	0.87±0.05
τ [ns]	**1.33**	**0.65**	**1.42**	**0.19**	τ [ns]	**1.77**	**0.65**	**1.15**	**0.39**
R2	0.99	0.99	0.99	0.99	R^2	0.99	0.99	1.00	0.99

Bold values represent tunica intima and tunica media: the innermost two layers of the wall of an artery

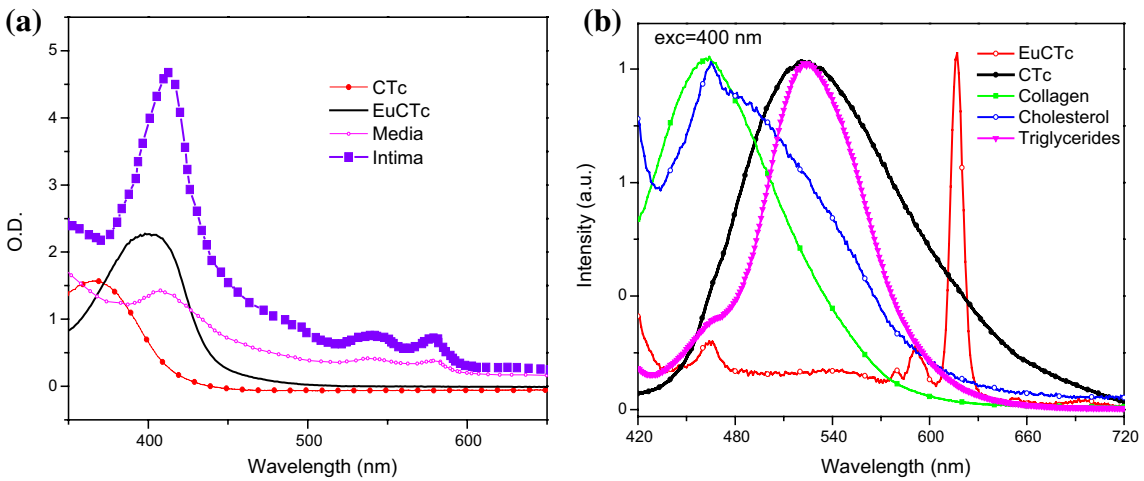

Fig. 3 **a** Absorption emission spectra of media and intima of an atherosclerotic aorta, and the Chlorotetracycline (CTc) and Europium Chlorotetracycline complex (EuCTc) (**b**) the emission of Europium Chlorotetracycline (EuCTc) complex, Chlorotetracycline (CTc) and cholesterol, TG and collagen obtained with excitation at 400 nm in function of the EuCTc concentration in each solution

huge energy transfer with collagen indicating that the properties of many tissues can be investigated using EuCTc as a fluorescent marker.

Previous studies have shown an interaction of tetracycline with the phospholipid [49]. This effect indicates that Europium Chlortetracycline could be retained in the artery walls facilitating the optical diagnosis. Europium complexes may offer new possibilities for target recognition and feedback-controlled safe tissue of coronary arteries. The emission peak of EuCTc is separated by enough spectral distance from the endogenous fluorophores. This feature can be applied to avoid the overlap between excitation and emission spectra of fluorophore itself or emission from biological matrix. Here measurements at 400 nm are

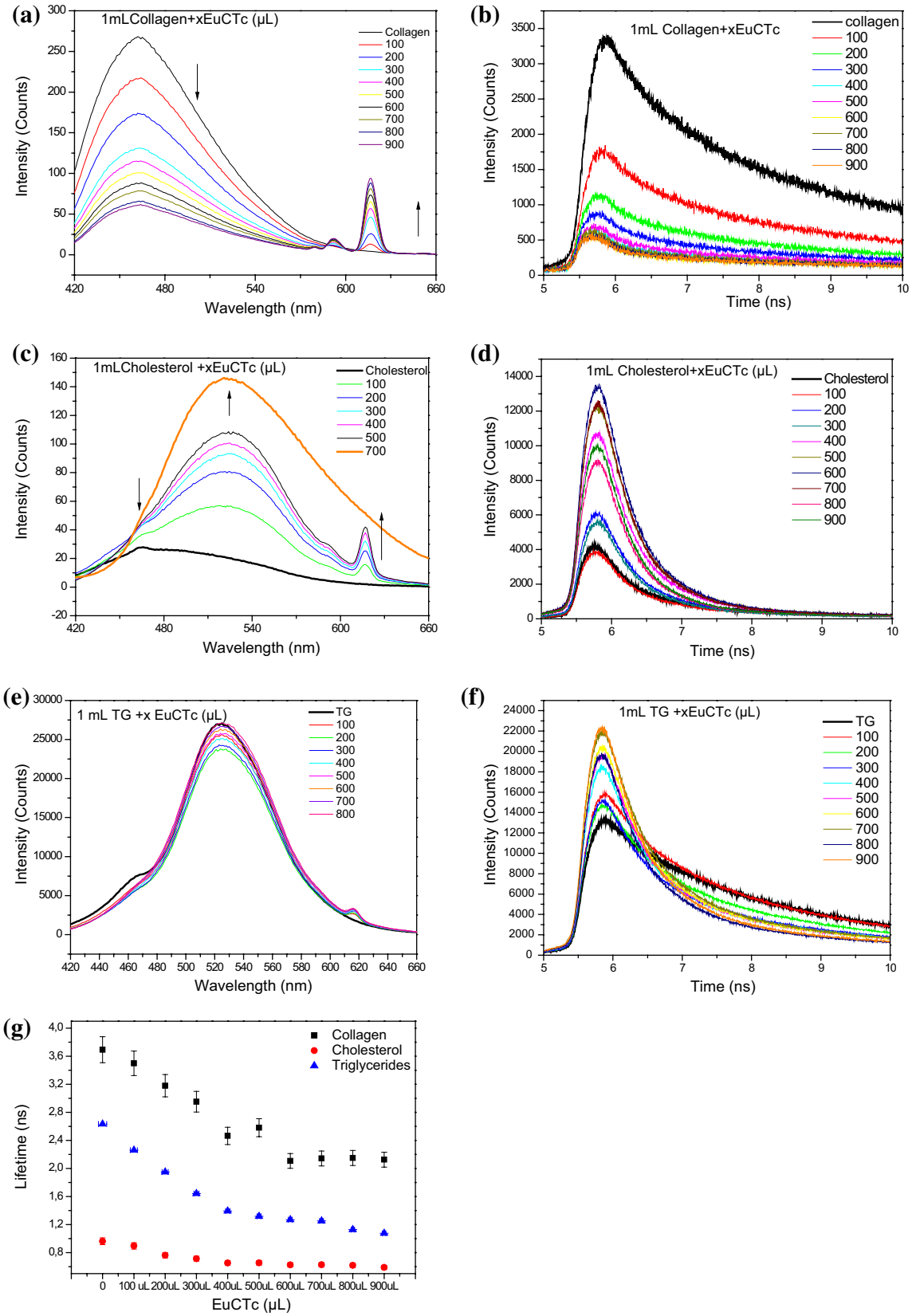

Fig. 4 Fluorescence spectra and fluorescence lifetime decays, obtained with excitation around 400 nm in the presence of variable amounts of EuCTc concentrations added to **a, b**: collagen solutions; **d, e**: cholesterol solutions; **e, f**: TG solutions. The EuCTc solution was added from 100 to 900 µL in 1 mL in each solution. **g** Collagen, cholesterol and TG averaged lifetimes obtained fitting decay times by two exponentials in function of EuCTc concentration in solutions

superficial, and just report on the immediate few hundred microns. The two-photon excitation of ultrashort pulse lasers (Ti: Sapphire) could improve investigation in very thick and large tissues.

Here we prepared EuCTc complex but Europium Tetracycline complex is currently commercialized (Sigma-02816), facilitating new studies and applications.

Conclusions

Atherosclerotic aortas stained with EuCTc and EuCTcMg showed significantly shorter emission lifetimes than normal aortas due to FRET between aorta fluorophores—mainly collagen, cholesterol and TG and Europium complexes. These results and the aforementioned studies provide encouraging data to support the concept that FLIM analysis using 405 nm excitation and EuCTc administration can sensitively identify atheroma.

Acknowledgments The authors acknowledge the National Institute of Science and Technology on Photonics Applied to Cell Biology (INFABIC) at the State University of Campinas for granting access to equipment and for providing assistance in this study. INFABIC is co-funded by Fundação de Amparo a Pesquisa do Estado de São Paulo (FAPESP) (08/57906-3) and Conselho Nacional de Desenvolvimento Cientifico e Tecnológico (CNPq) (573913/2008-0), and the FAPESP 2014/06960-9 (Sources of Funding).

Funding This study was funded by Fapesp (Grant Number 2014/06960-9).

Compliance with ethical standards

Conflict of interest None of the authors have conflict of interest in regards to the content of this manuscript.

Ethical approval All applicable international, national, and/or institutional guidelines for the care and use of animals were followed. Ethics Committee of UNIFESP (Protocol no. 0327/12).

References

1. Castelli WP (1996) Lipids, risk factors and ischaemic heart disease. Atherosclerosis 124:S1–S9
2. Ross R (1999) Mechanisms of disease–Atherosclerosis—an inflammatory disease. N Engl J Med 340:115–126
3. Ross JS, Stagliano NE, Donovan MJ, Breitbart RE, Ginsburg GS (2001) Atherosclerosis and cancer—common molecular pathways of disease development and progression. Ann N Y Acad Sci 947:271–293
4. Mahia-Casado P, Garcia-Orta R, Gomez de Diego JJ, Barba-Cosials J, Rodriguez-Palomares JF, Aguade-Bruix S (2015) Update on Cardiac Imaging Techniques 2014. Revista Espanola De Cardiologia 68:129–135
5. Aghayev A, Murphy DJ, Keraliya AR, Steigner ML (2016) Recent developments in the use of computed tomography scanners in coronary artery imaging. Expert Rev Med Devices 13:545–553
6. Vijayalaxmi M, Fatahi OS (2015) Magnetic resonance imaging (MRI): a review of genetic damage investigations. Mutat Res Rev Mutat Res 764:51–63
7. Sarikaya I (2015) Cardiac applications of PET. Nucl Med Commun 36:971–985
8. Escolar E, Weigold G, Fuisz A, Weissman NJ (2006) New imaging techniques for diagnosing coronary artery disease. Can Med Assoc J 174:487–495
9. Blankstein R (2012) Cardiology patient page. Introduction to noninvasive cardiac imaging. Circulation 125:e267
10. Dunn JP, Huizinga MM, See R, Irani WN (2010) Choice of imaging modality in the assessment of coronary artery disease risk in extreme obesity. Obesity 18:1–6
11. Maarek JMI, Marcu L, Fishbein MC, Grundfest WS (2000) Time-resolved fluorescence of human aortic wall: use for improved identification of atherosclerotic lesions. Lasers Surg Med 27:241–254
12. Manolopoulos A, Vasileiou A, Kokkinos V, Athanasopoulos C, Agapitos E, Kavantzas N, Yova D (2000) Comparative studies of Laser Induced Fluorescence and Intravascular Ultrasound for the human coronary artery diagnosis of atherosclerosis. Optics and lasers in biomedicine and culture. Series of the international society on optics within life sciences. Vol 5, pp 316–323
13. Megens RTA, Bianchini M, Schmitt MMN, Weber C (2015) Optical imaging innovations for atherosclerosis research multiphoton microscopy and optical nanoscopy. Arterioscler Thromb Vasc Biol. 35:1339–1346
14. Sanz J, Fayad ZA (2008) Imaging of atherosclerotic cardiovascular disease. Nature 451:953–957
15. Sicchieri LB, Barioni MB, Silva MN, Monteiro AM, Figueiredo Neto AM, Ito AS, Courrol LC (2014) Atherosclerosis staging: imaging using FLIM technique. In: Proceedings SPIE 8947, imaging, manipulation, and analysis of biomolecules, cells, and tissues XII, 89472B (March 4, 2014). doi:10.1117/12.2040139
16. Arakawa K, Isoda K, Ito T, Nakajima K, Shibuya T, Ohsuzu F (2002) Fluorescence analysis of biochemical constituents identifies atherosclerotic plaque with a thin fibrous cap. Arterioscler Thromb Vasc Biol 22:1002–1007
17. Bartorelli AL, Leon MB, Almagor Y, Prevosti LG, Swain JA, McIntosh CL, Neville RF, House MD, Bonner RF (1991) Invivo human atherosclerotic plaque recognition by laser-excited fluorescence spectroscopy. J Am Coll Cardiol 17:B160–B168
18. Morguet AJ, Korber B, Abel B, Hippler H, Wiegand V, Kreuzer H (1994) Autofluorescence spectroscopy using a xecl excimer-laser system for simultaneous plaque ablation and fluorescence excitation. Lasers Surg Med 14:238–248
19. Sun Y, Sun Y, Stephens D, Xie H, Phipps J, Saroufeem R, Southard J, Elson DS, Marcu L (2011) Dynamic tissue analysis using time-and wavelength-resolved fluorescence spectroscopy for atherosclerosis diagnosis. Opt Express 19:3890–3901
20. Jo JA, Fang Q, Papaioannou T, Baker JD, Dorafshar AH, Reil T, Qiao JH, Fishbein MC, Freischlag JA, Marcu L (2006) Laguerre-based method for analysis of time-resolved fluorescence data: application to in-vivo characterization and diagnosis of atherosclerotic lesions. J Biomed Opt 11(2):021004. doi:10.1117/1.2186045
21. Marcu L, Fishbein MC, Maarek JMI, Grundfest WS (2001) Discrimination of human coronary artery atherosclerotic lipid-rich lesions by time-resolved laser-induced fluorescence spectroscopy. Arterioscler Thromb Vasc Biol 21:1244–1250
22. Anderssonengels S, Johansson J, Svanberg K, Svanberg S (1991) Fluorescence imaging and point measurements of tissue—applications to the demarcation of malignant-tumors and atherosclerotic lesions from normal tissue. Photochem Photobiol 53:807–814

23. Phipps J, Sun Y, Saroufeem R, Hatami N, Fishbein MC, Marcu L (2011) Fluorescence lifetime imaging for the characterization of the biochemical composition of atherosclerotic plaques. J Biomed Opt 16:096018
24. Marcu L, Fang QY, Jo JA, Papaioannou T, Dorafshar A, Reil T, Qiao JH, Baker JD, Freischlag JA, Fishbein MC (2005) In vivo detection of macrophages in a rabbit atherosclerotic model by time-resolved laser-induced fluorescence spectroscopy. Atherosclerosis 181:295–303
25. Phipps J, Sun Y, Saroufeem R, Hatami N, Marcu L (2009) Fluorescence lifetime imaging microscopy for the characterization of atherosclerotic plaques. In: Kollias N, Choi B, Zeng H, Malek RS, Wong BJF, Ilgner JFR, Gregory KW, Tearney GJ, Marcu L, Hirschberg H, Madsen SJ (eds) Proceedings SPIE 7161, photonic therapeutics and diagnostics V, 71612G (February 23, 2009). doi:10.1117/12.813087
26. Ashjian P, Elbarbary A, Zuk P, DeUgarte DA, Benhaim P, Marcu L, Hedrick MH (2004) Noninvasive in situ evaluation of osteogenic differentiation by time-resolved laser-induced fluorescence spectroscopy. Tissue Eng 10:411–420
27. Lindgren I, Raekalli J (1966) Accumulation of tetracyclines in atherosclerotic lesions of human aorta. Acta Pathol Microbiol Scand 66:323–326
28. Golub LM, Greenwald RA (2011) Clinical applications of non-antibacterial tetracyclines. Part II preface. Pharmacol Res 64:549–550
29. Donohue J, Trueblood KN, Webster MS, Dunitz JD (1963) Crystal structure of aureomycin (chlortetracycline) hydrochloride—configuration, bond distances and conformation. J Am Chem Soc 85:851
30. Welch H (1953) About the chemically descriptive generic terms for aureomycin (chlortetracycline) and terramycin (oxytetracycline). Antibiot Chemother 3:659–662
31. Durckheimer W (1975) Tetracyclines—chemistry, biochemistry, and structure–activity relations. Angew Chem Int Ed Engl 14:721–734
32. Benet LZ, Goyan JE (1966) Thermodynamics of chelation by tetracyclines. J Pharm Sci 55:1184–1190
33. Coibion C, Laszlo P (1979) Binding of the alkali-metal cations to tetracycline. Biochem Pharmacol 28:1367–1372
34. Courrol LC, Silva FRD, Gomes L, Vieira ND (2007) Energy transfer study of europium-tetracycline complexes. J Lumin 122:288–290
35. Courrol LC, Samad RE (2008) Applications of europium tetracycline complex: a review. Curr Pharm Anal 4:238–248
36. Georges J, Ghazarian S (1993) Study of europium-sensitized fluorescence of tetracycline in a micellar solution of triton x-100 by fluorescence and thermal lens spectrometry. Anal Chim Acta 276:401–409
37. Hirschy LM, Vangeel TF, Winefordner JD, Kelly RN, Schulman SG (1984) Characteristics of the binding of europium(iii) to tetracycline. Anal Chim Acta 166:207–219
38. Izquierdo P, Gomezhens A, Perezbendito D (1994) Study of the Eu(iii)-tetracycline-thenoyltrifluoroacetone system by using the stopped-flow mixing technique—determination of tetracycline in serum. Anal Chim Acta 292:133–139
39. Courrol LC, Sicchieri LB, Silva DC (2013) Cholesterol accumulation in the cornea and in the aorta: imaging using europium chlortetracycline complex fluorescent probe. In: Conference on optical diagnostics and sensing XIII-toward point-of-care diagnostics, San Francisco, CA
40. Teixeira LDS, Grasso AN, Monteiro AM, Figueiredo Neto AM, Vieira ND Jr, Gidlund M, Courrol LC (2010) Enhancement on the Europium emission band of Europium chlortetracycline complex in the presence of LDL. Anal Biochem 400:19–24
41. da Silva MN, Sicchieri LB, de Oliveira Silva FR, Andrade MF, Courrol LC (2014) Liquid biopsy of atherosclerosis using protoporphyrin IX as a biomarker. Analyst 139:1383–1388
42. Keijzer M, Richardskortum RR, Jacques SL, Feld MS (1989) Fluorescence spectroscopy of turbid media—autofluorescence of the human aorta. Appl Opt 28:4286–4292
43. Murata K, Motayama T, Kotake C (1986) Collagen types in various layers of the human aorta and their changes with the atherosclerotic process. Atherosclerosis 60:251–262
44. Dos Santos I, Mazeres S, Freche M, Lacout J-L, Sautereau A-M (2008) FRET: a tool to study the interaction between apatite and collagen? Mater Lett 62:4377–4379
45. Chou KF, Dennis AM (2015) Forster resonance energy transfer between quantum dot donors and quantum dot acceptors. Sensors 15:13288–13325
46. Hiltunen TP, Luoma JS, Nikkari T, Yla-Herttuala S (1998) Expression of LDL receptor, VLDL receptor, LDL receptor-related protein, and scavenger receptor in rabbit atherosclerotic lesions—marked induction of scavenger receptor and VLDL receptor expression during lesion development. Circulation 97:1079–1086
47. Matthaus C, Cicchi R, Meyer T, Lattermann A, Schmitt M, B.F.M. Romeike, Krafft C, Dietzek B, Brehm BR, Pavone FS, Popp J (2014) Multimodal nonlinear imaging of atherosclerotic plaques differentiation of triglyceride and cholesterol deposits. J Innov Opt Health Sci 7:10
48. San Antonio JD, Di Lullo GA, Sweeney SM, Korkko J, Ala-Kokko L (2001) Mapping the ligand-binding sites and disease-associated mutations on the most abundant protein in the human-type I collagen Mol Biol Cell 12:9A–9A
49. Caminati G, Focardi C, Gabrielli G, Gambinossi F, Mecheri B, Nocentini M, Puggelli M (2002) Spectroscopic investigation of tetracycline interaction with phospholipid Langmuir–Blodgett films. Mat Sci Eng C-Biomim Supramol Sys 22:301–305